

Electronic Supplementary Information

**Studying the effect of the degree of functionalization towards the thermal  
rearrangement temperature of *ortho*-allyloxypolyimide membranes**

David Meis<sup>1</sup>, Alberto Tena<sup>1</sup>, Silvio Neumann<sup>1</sup>, Prokopios Georgopoulos<sup>1</sup>, Thomas Emmeler<sup>1</sup>,  
Sergey Shishatskiy<sup>1</sup>, Sofia Rangou<sup>1</sup>, Volkan Filiz<sup>1</sup> and Volker Abetz<sup>1,2</sup>

<sup>1</sup>Helmholtz-Zentrum Geesthacht, Institute of Polymer Research, Max-Planck-Str.1, 21502  
Geesthacht, Germany

<sup>2</sup>University of Hamburg, Institute of Physical Chemistry, Martin-Luther-King Platz 6, 20146  
Hamburg, Germany

\*correspondence to: volkan.filiz@hzg.de, volker.abetz@hzg.de

## Structure and Thermal Characterization

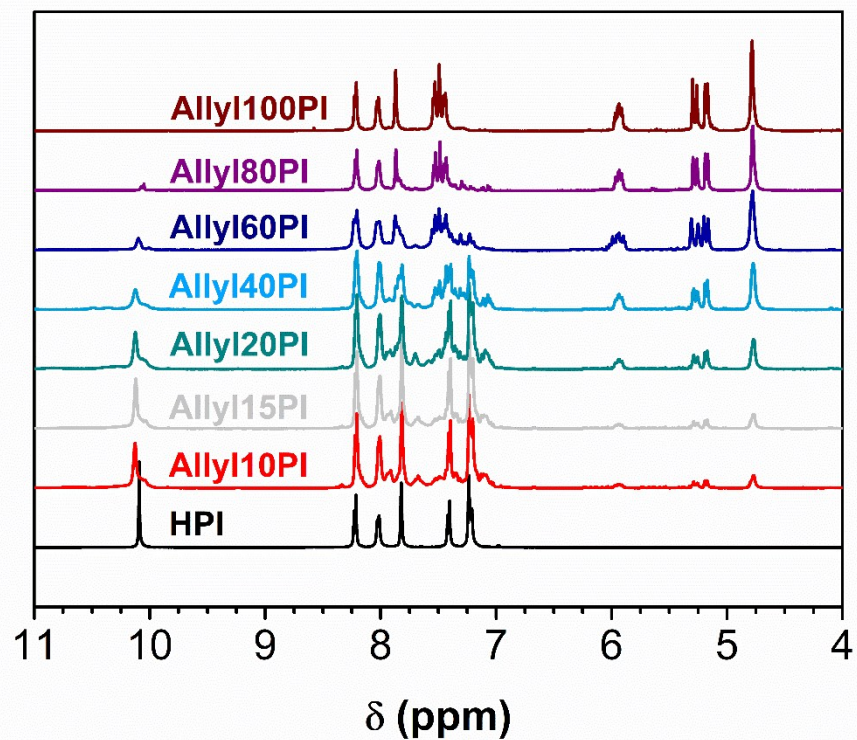


**Figure S1.** Stacked <sup>1</sup>H-solution-state NMR (DMSO-d<sub>6</sub>, 500 MHz) spectra of all synthesized polyimides with respect to their degree of allylation.

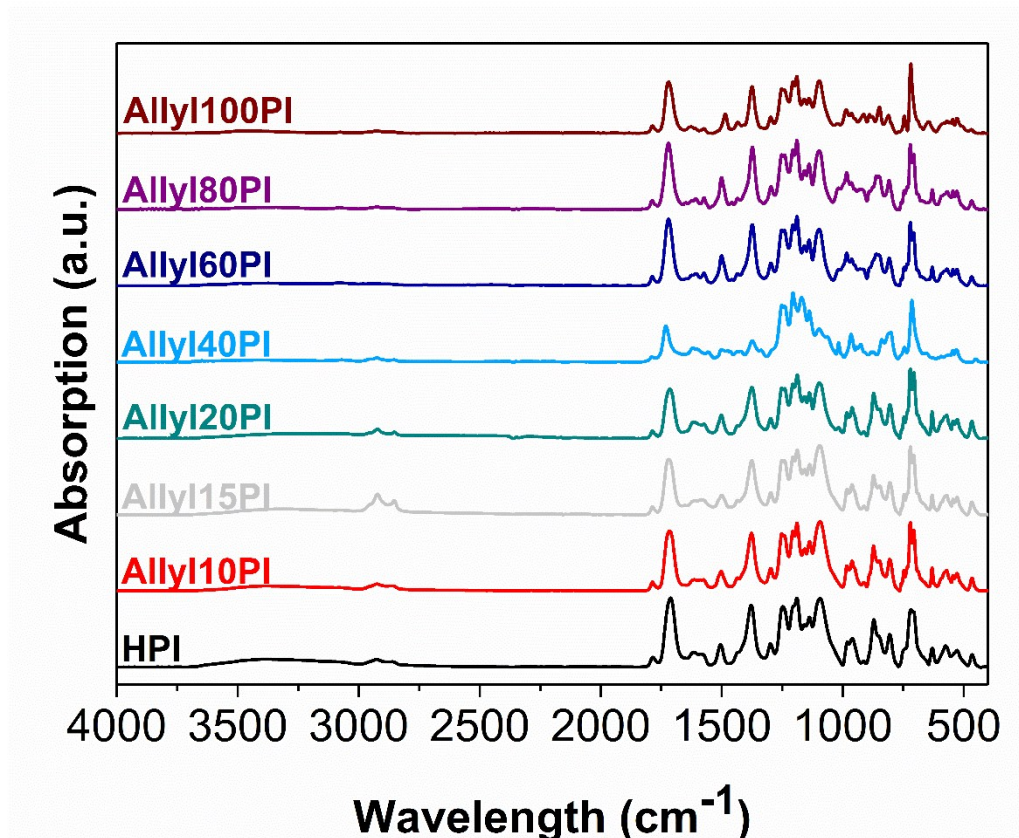


**Figure S2.** FT-IR spectra of all synthesized polyimides with respect to their degree of allylation.

All FT-IR spectra of the modified polyimides showed characteristic absorption bands for polyimides at  $1786\text{ cm}^{-1}$  (symmetric C=O stretching vibration band) and at  $1716\text{ cm}^{-1}$  (asymmetric C=O stretching vibration band). The transverse stretching C-N-C band was found at  $1102\text{ cm}^{-1}$  as well as the out-of-plane bending of the C-N-C group at  $720\text{ cm}^{-1}$  and the characteristic asymmetric stretching vibration band at  $1377\text{ cm}^{-1}$  for the C-N group. In addition, the C-F group was identified at  $1150\text{--}1250\text{ cm}^{-1}$ . The successful allylation was confirmed due to the appearance of a characteristic sharp C-O-C symmetric stretching band of the allylphenylether group at  $1031\text{ cm}^{-1}$  and the stretching vibration of the vinyl (=C-H) group at  $3083\text{ cm}^{-1}$ . The broad band in the region from  $3200\text{--}3600\text{ cm}^{-1}$  was attributed to the O-H vibration of the unmodified *ortho*-hydroxy groups.

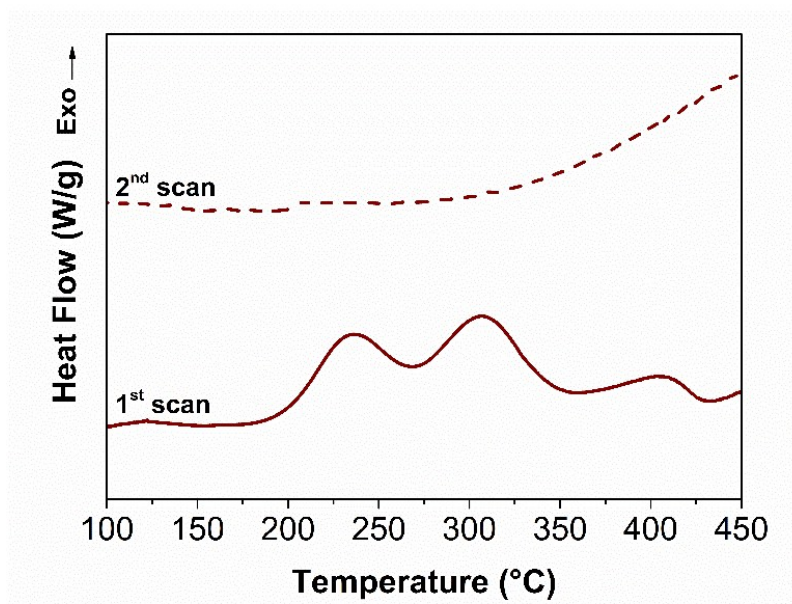


**Figure S3.** DSC curve of Allyl100PI. Heating rate was 5 °C min<sup>-1</sup>.

**Table S1.** Solubility of the synthesized polyimide films with respect to their degree of allylation.

Degree of Allylation (%)	NMP, DMF, DMAC	DMSO	THF	Acetone	EtOH, MeOH	CHCl <sub>3</sub>	H <sub>2</sub> O
0	++	++	+	++	-	-	-
10	++	++	+	++	-	-	-
15	++	++	+	++	-	-	-
20	++	++	+	++	-	-	-
40	++	++	+	++	-	+	-
60	++	++	+	++	-	+	-
80	++	++	+	++	-	+	-
100	++	++	+	++	-	++	-

++: soluble; +: partially soluble or swelling; -: insoluble.

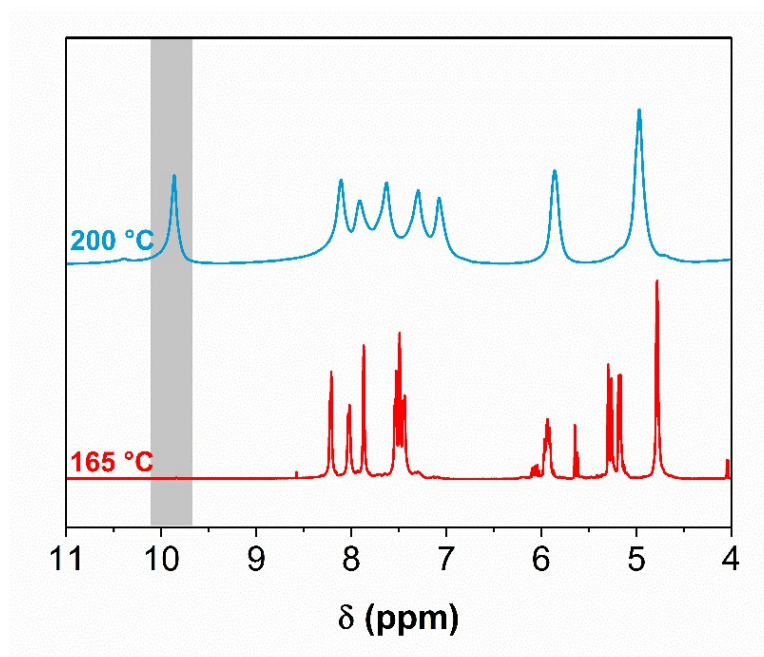


**Figure S4.**  $^1\text{H}$ -solution-state NMR (DMSO- $d_6$ , 500 MHz) spectra of all Allyl100PI after annealing for 24 h at 165 °C and 10 h at 200 °C, respectively.

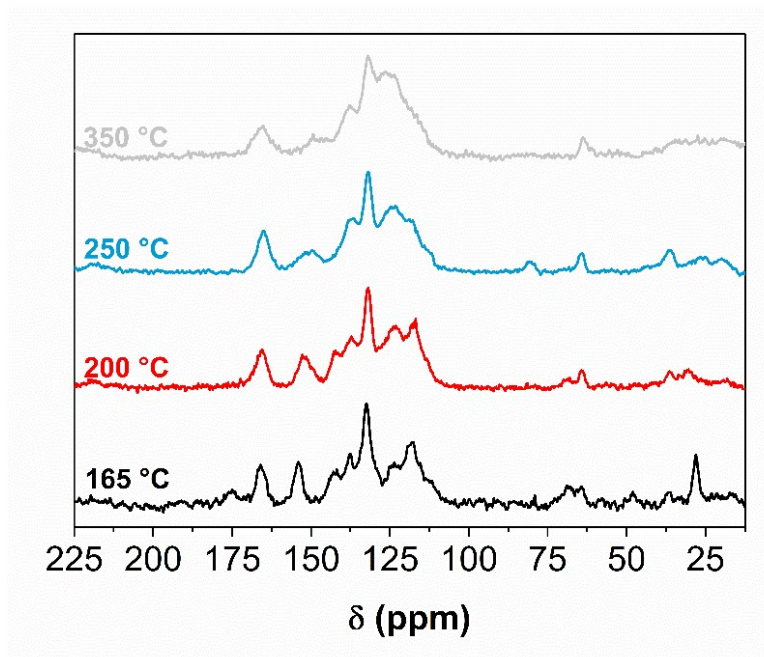


**Figure S5.**  $^{13}\text{C}$ -solid-state NMR (CPMAS) spectra of Allyl100PI after annealing at 165 °C, 200 °C, 250 °C and 350 °C.

**Table S2.** Gel-fraction and swelling ratio of the synthesized polyimides determined after isothermal treatments at 250 °C for 10 h and 350 °C for 2 h using DMF as a solvent.

Degree of Allylation	Gel-fraction (%)		Swelling (%)	
	TR250	TR350	TR250	TR350
10	96	100	269	69
15	96	100	228	64
20	97	100	215	59
40	97	100	209	50
60	98	100	128	60
80	99	100	111	65
100	100	100	74	95

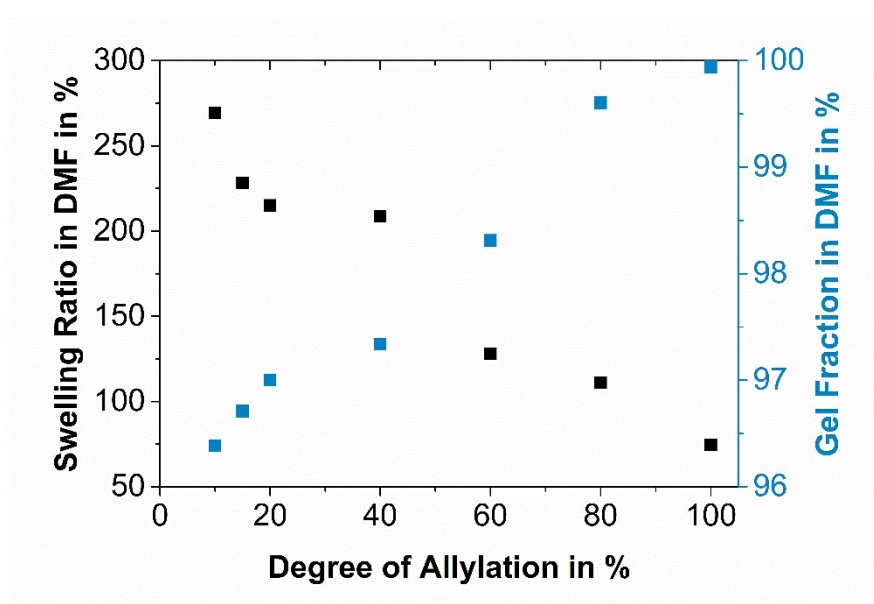


**Figure S6.** Gel-fraction and swelling ratio of the synthesized polyimides determined after the isothermal treatments at 250 °C for 10 h in DMF.

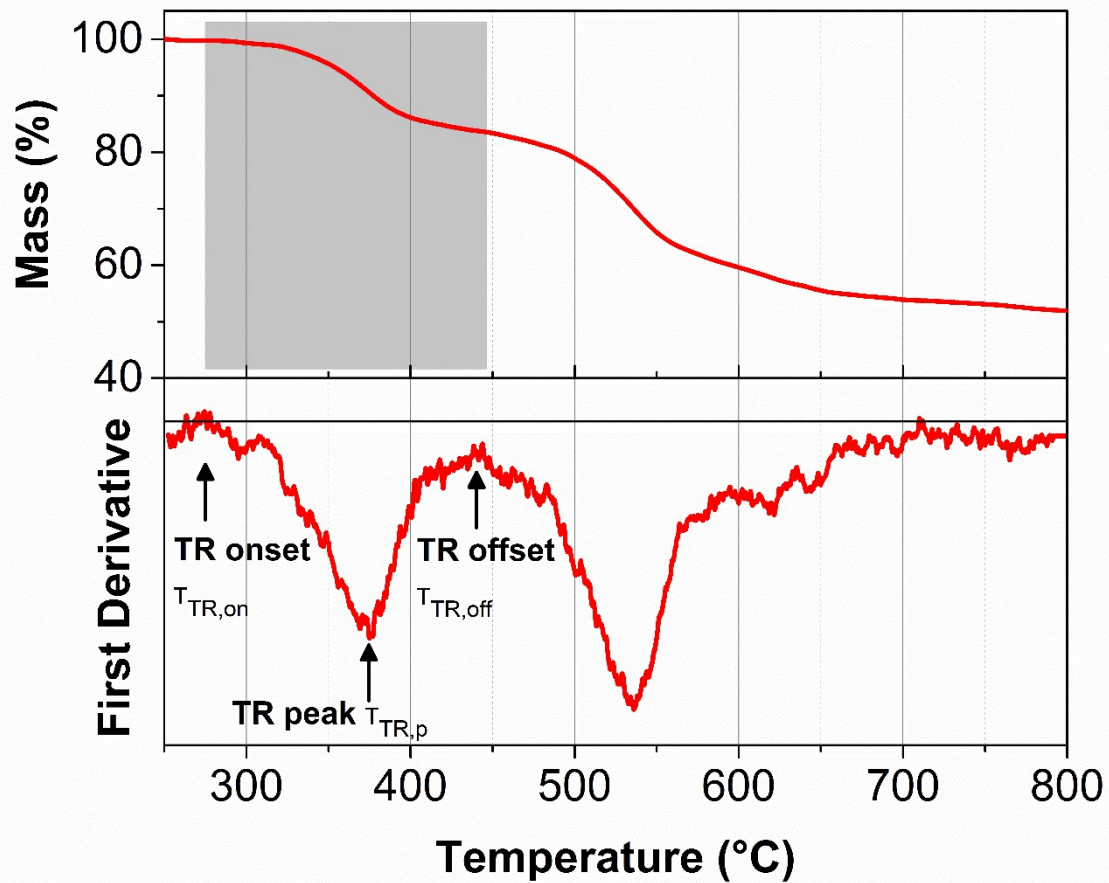


**Figure S7.** TGA-Curve (top) and the first derivative (bottom) of Allyl40PI, as well as the TR onset, peak and offset temperature determination.

## Monomer modification

The synthetic route for the monomer modification is shown in scheme 1.

## Monomer protection

HAB (4.3 g; 20 mmol) and phthalic acid anhydride (7.4 g; 50 mmol) were suspended in diethyl ether (40 mL) in a round-bottom flask and stirred in an ice bath under argon for 24, whereas the temperature of the ice bath increased to room temperature. The solid was filtered off, washed several times with diethyl ether, and then dried under vacuum at 80 °C.

The azeotropic imidization route was used to convert the phthalic acid anhydride protected diamine (Paa-HAB) in its amic acid form. Therefore, Paa-HAB (8.5 45 g; 20 mmol) was dissolved in 10 mL NMP and *o*-xylene (8.0 mL) was added to the vigorously stirred solution. The temperature was raised to 180 °C and kept for 6 h to promote complete imidization. The formed water was removed as an *o*-xylene/water azeotropic mixture from the solution and residual *o*-xylene was removed under reduced pressure. The phthalimide-protected diamine (PI-HAB) was precipitated in deionized water and washed several times with distilled water and methanol. The PI-HAB was then dried under vacuum at 100 °C for 24 h.

## Synthesis of the allyl functionalized polymers via post-polymerization modification

The *ortho*-hydroxy groups of the protected diamine were converted to the corresponding allylic ether group by a Williamson-ether type synthesis (see Scheme S1). PI-HAB (5.3 g; 1. mmol) was dissolved in anhydrous DMF (8.0 mL) in a three-necked round bottom flask under argon atmosphere at 60 °C. The activation of the hydroxy groups was carried out by adding dried potassium carbonate (2.3 g; 2. mmol) to the mixture under stirring. After 4 h the allyl bromide (4.5 mL; 5 mmol) was added to the solution. The mixture was stirred under these conditions for two hours, whereas the same amount of potassium carbonate and allyl bromide were added after 4 h again. After 24 h the mixture was cooled down to room temperature and precipitated in deionized water. The allylated-protected diamine (PI-HAB Allyl) was repeatedly washed with water and methanol and dried in a vacuum oven at 120 °C for 72 h.

## Monomer deprotection

The phthalimide protected allylated diamine (PI-HAB Allyl) was deprotected by means of hydrazine addition under cleavage of phthalhydrazide. PI-HAB Allyl (5.9 g; 1 mmol) was suspended in ethanol (10 mL) under argon and cooled in an ice bath. An aqueous solution of hydrazine (35 wt.%) (0.21 mL; 2.4 mmol) was added dropwise. During the synthesis, the suspension turned into a clear solution due to the addition of hydrazine and became turbid again very quickly because of the phthalhydrazide formation. The solid was filtered off after 2 h and washed with ethanol several times. The ethanol was evaporated under reduced pressure at room temperature. The residuals were suspended in methanol and the solid was filtered off. The methanol was evaporated under reduced pressure followed by several washing steps in water, followed by recrystallization from ethylacetate.

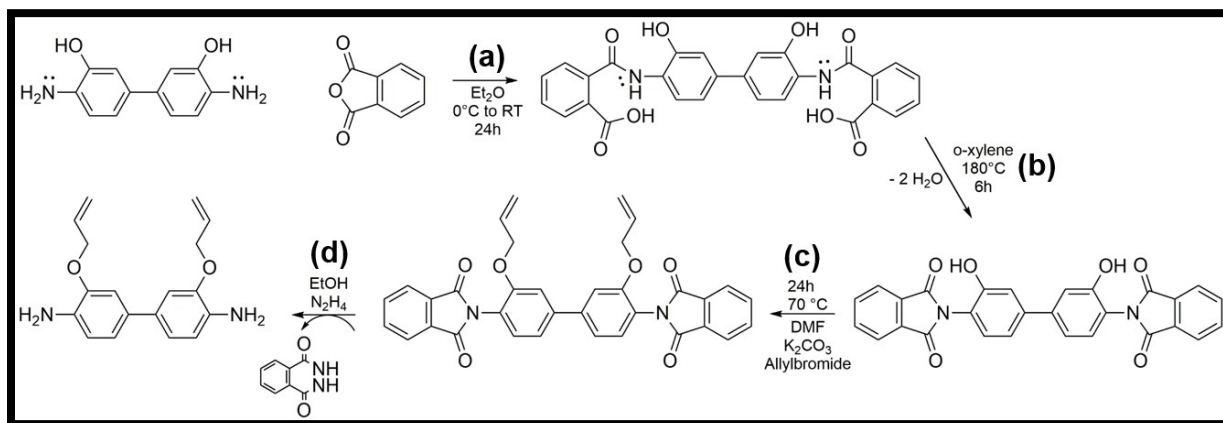
## Synthesis of 6FDA-HAB precursor polymer

The *ortho*-allyloxy polyimide precursor based on HAB, HAB-Allyl and 6FDA was synthesized by a two-step polycondensation reaction.

The procedure for CoPo-Allyl10PI is described as follows. HAB (4.3 g; 18 mmol) and HAB-Allyl (0.59 g; 2 mmol) was charged to a three-necked flask, equipped with a mechanical stirrer and a gas inlet, and stirred in 15 mL of NMP at room temperature under argon until completely dissolved. 6FDA (8.8 g; 20 mmol) and additional 15 mL of NMP were then added and the resulting mixture was cooled to 0 °C and stirred overnight, whereas the temperature of the ice bath increased to room temperature.

The azeotropic imidization route was used to convert the poly (amic acid) to polyimide. Therefore, *p*-xylene (8 mL) was added to the vigorously stirred viscous solution. The temperature was raised to 160 °C and kept for 8 h to promote complete imidization. The formed water was removed as a *p*-xylene/water azeotropic mixture from the solution and residuals of the *p*-xylene were removed under reduced pressure. The polymer was precipitated in

deionized water and washed several times with distilled water and methanol. The polymer was then dried under vacuum at 100 °C.



**Scheme S1.** Synthesis route for the monomer modification. (a) Protection: HAB (diamine), phthalic acid anhydride, Et<sub>2</sub>O, 0 °C, 24 h; (b) Imidization: *o*-xylene, 180 °C, 6 h; (c) Alkylation: Allylbromide, K<sub>2</sub>CO<sub>3</sub>, DMF, 70 °C, 24 h; (d) Deprotection: Hydrazine, ethanol, 0 °C, 2 h.

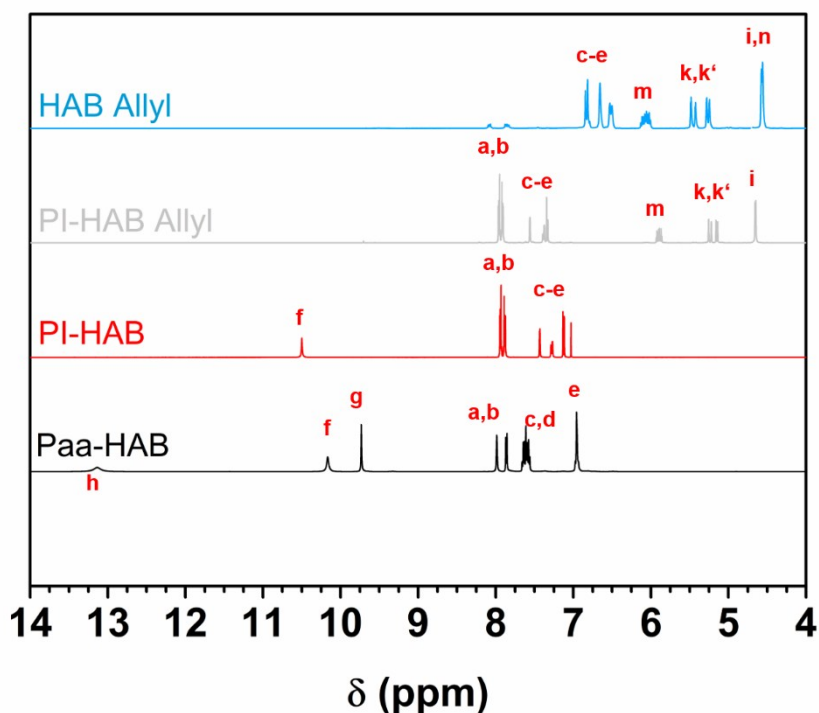
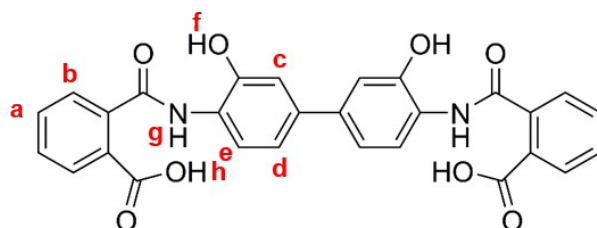
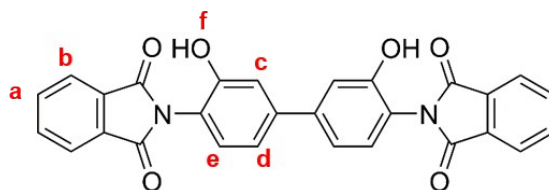


**Figure S8.** Stacked  $^1\text{H}$ -solution-state NMR (DMSO- $d_6$ , 500 MHz) spectra of the phtalic acid anhydride protected HAB diamine in its amic acid form (black), imidized form (red) and after the allylation (grey) as well as after deprotection (blue).

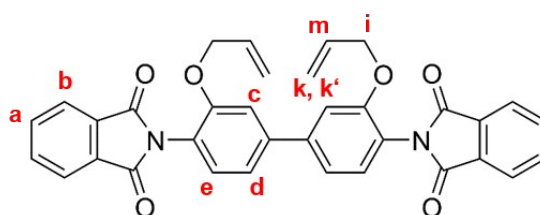
#### Overview of the new monomers (chemical structure and $^1\text{H}$ -NMR characterization)



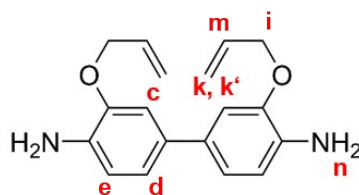
Paa-HAB:  $^1\text{H}$  NMR (DMSO- $d_6$ , ppm); For specific assignments see Figure S8: 13.2 (br s, 2 H, carboxyl, **h**); 10.2 (s, 2 H, hydroxyl, **f**); 9.5 (s, 2 H, amide, **g**); 7.7-7.9 (m, 8 H, aromatic, **a**, **b**); 7.5-7.7 (m, 4 H, aromatic, **c**, **d**); 6.9 (s, 2 H, aromatic, **e**).



PI-HAB:  $^1\text{H}$  NMR (DMSO- $d_6$ , ppm); For specific assignments see Figure S8: 10.4 (s, 2 H, hydroxyl, **f**); 7.7-7.9 (m, 8 H, aromatic, **a, b**); 7.0-7.5 (m, 6 H, aromatic, **c-e**).



PI-HAB Allyl:  $^1\text{H}$  NMR (DMSO- $d_6$ , ppm); For specific assignments see Figure S8: 7.7-7.9 (m, 8 H, aromatic, **a, b**); 7.0-7.3 (m, 6 H, aromatic, **c-e**); 5.8-6.0 (m, 2 H, vinyl, **m**); 5.3-5.5 (dd, 4 H, vinyl, **k,k'**); 4.5 (s, 4 H, allylic, **i**).



HAB Allyl:  $^1\text{H}$  NMR (DMSO- $d_6$ , ppm); For specific assignments see Figure S8: 7.4-7.9 (m, 6 H, aromatic, **c-e**); 5.8-6.0 (m, 2 H, vinyl, **m**); 5.3-5.6 (dd, 4 H, vinyl, **k,k'**); 4.5 (s, 4 H, allylic, **i**); 4.5 (s, 4 H, amine, **n**).

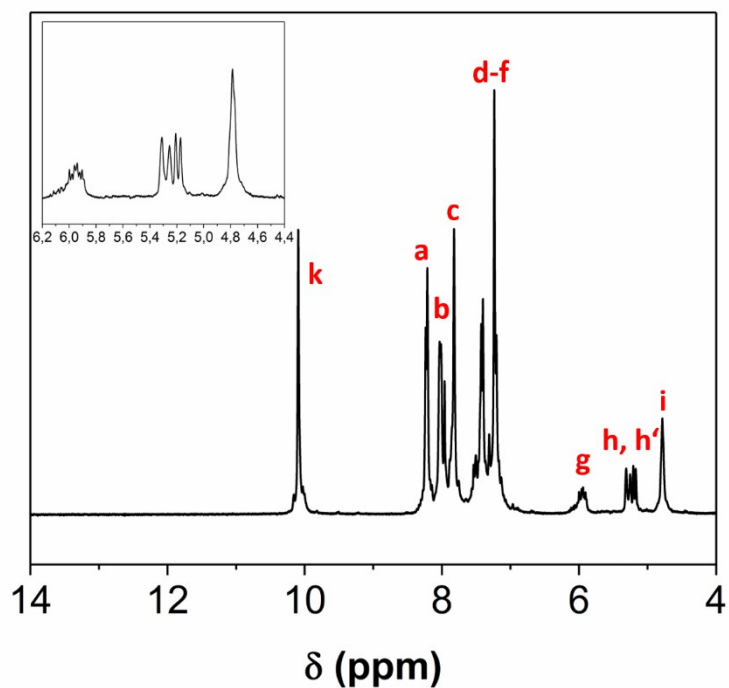
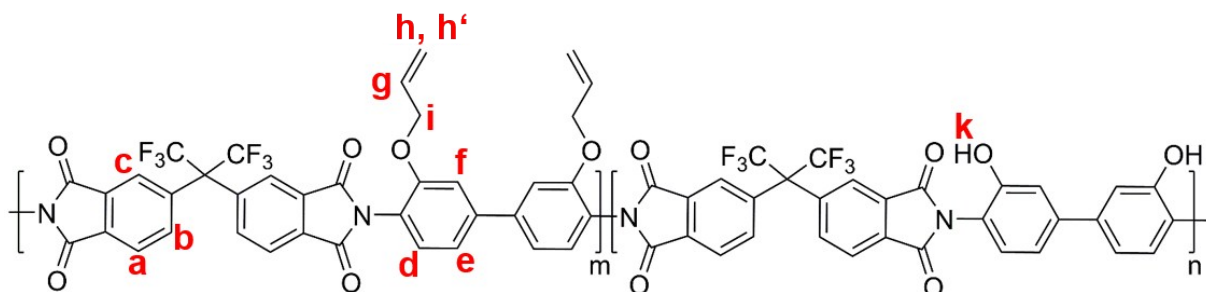


**Figure S9.**  $^1\text{H}$ -solution-state NMR ( $\text{DMSO-d}_6$ , 500 MHz) spectra of the copolymerized CoPo-Allyl15PI.



CoPo-Allyl15PI ( $m = 15$ ;  $n = 85$ ):  $^1\text{H}$  NMR ( $\text{DMSO-d}_6$ , ppm); For specific assignments see Figure S9: 10.1 (s, 1.7 H, hydroxyl, **k**); 7.2-8.3 (m, 12 H, aromatic, **a-f**); 5.8-6.2 (m, 0.3 H, vinyl, **g**); 5.6-5.8 (m, 0.6 H, vinyl, **h, h'**); 4.4 (s, 0.6 H, allylic, **i**).

## Thermal Characterization of the synthesized allylated copolymers

The copolymers with ratios of 10, 15 and 100% of allylated HAB and 90, 85 and 0% of HAB, respectively, as a diamine compound were investigated by means of TGA measurements. This has been done in order to check, if the TR process occurs in the same temperature range as observed for the corresponding post-polymerization modified materials with 10, 15 and 100% of allyloxy groups. While the post-polymerization modified materials show TR onset temperatures of 280 °C and peak temperatures of 391 and 373 °C for the Allyl10PI and Allyl15PI, the corresponding copolymerized polymers CoPo-Allyl10PI and CoPo-Allyl15PI show a significantly higher TR onset temperature of 360 °C and peak temperatures of 400 °C (CoPo-Allyl10PI) and 420 °C (CoPo-Allyl15PI). Moreover, the copolymer containing 10% of allylated units shows a lower TR peak temperature compared to the material with 15% of allylated HAB units, which is in comparison to the post-polymerization modified materials in a reversed order. The 100% allylated polyimide shows a TR onset temperature of 370 °C for the copolymerized and 360 °C for the post-polymerization modified material, and very similar peak temperatures of 420 and 426 °C, respectively. These findings reveal a tremendous effect of the allyloxy distribution in the polymer. Both, the Allyl100 and CoPo-Allyl100PI, show nearly identical results as their chemical structure are the same and differ only in the synthesis route. The copolymers with 10 and 15% of allyloxy units however, show a strong effect of the allyl distribution. Using a post-polymerization modification route, it can be assumed that the allylation of the hydroxyl groups occurs randomly, whereas the statistical chance of having mono allylated repetition units is at the highest. In the copolymerized materials there are only fully allylated and non-allylated repetition units. Since the pristine polymer as well as the 100% allylated homopolymers, with its non- and fully allylated units, have high TR temperatures above 400 °C, while Allyl10 and Allyl15PI have also mono allylated repetition units, each repeating unit of the copolymerized material thermally rearranges to its corresponding PBO form at temperatures according to the homopolymers. The post-polymerization allylated material with its mono allylated repetition units rearranges at lower temperatures, amongst

other due to the spacer effect, which is presumably higher, since more repetition units contain allyloxy groups compared to CoPo-Allyl10- and CoPo-Allyl15PI.

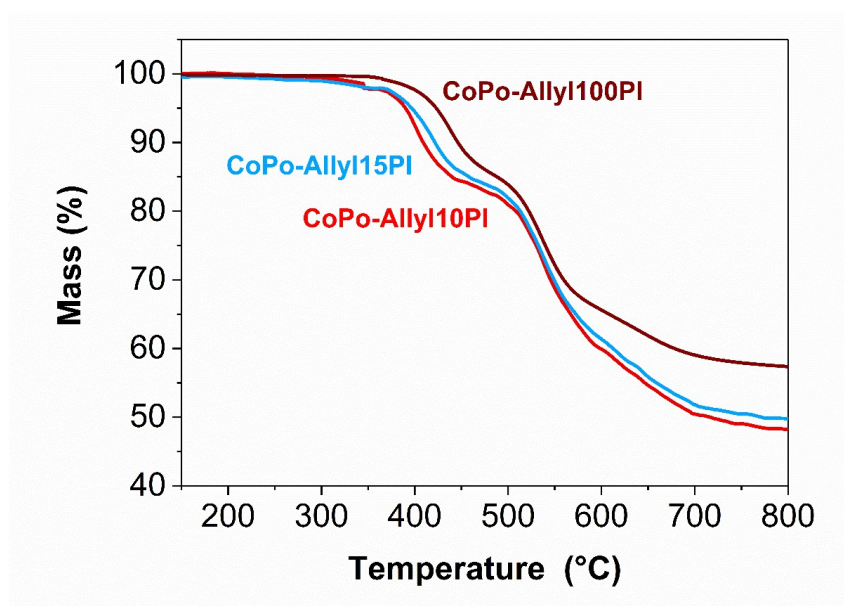


**Figure S10.** TGA curve of CoPo-Allyl10PI (red), CoPo-Allyl15PI (grey) and CoPo-Allyl100PI (brown). The heating rate was 5 °C min<sup>-1</sup>.

### Dielectric Spectroscopy

In Figure S8 the relaxation time  $\tau_{\max}$  is plotted as a function of the inverse temperature. The relaxation time was calculated by fitting the Havriliak-Negami equation (equation S1) with the software WinFit from Novocontrol for the  $\beta$ -relaxation process in the temperature range of 200 – 300 °C<sup>1-3</sup>.

$$\varepsilon_{HN}^* = \varepsilon_{\infty} + \sum_{k=1}^m \frac{\Delta\varepsilon_k}{[1 + (i\omega\tau_{HN,k})^{\alpha_k}]^{\beta_k}} \quad (\text{eq. S1})$$

with  $m$  modes and the dielectric strength  $\Delta\varepsilon_k$  of the  $k$ th mode.  $\varepsilon_{\infty}$  describes the permittivity in the high frequency limit and  $\tau_{HN,k}$  the characteristic relaxation time of the corresponding process. The parameters  $\alpha_k$  ( $0 < \alpha_k$ ) and  $\beta_k$  ( $\beta_k \leq 1$ ) describe the asymmetry and the broadening of the dielectric loss  $\varepsilon''$  as a function of angular frequency  $\omega = 2\pi f$ , respectively.

All materials showed an Arrhenius behavior for the  $\beta$  process<sup>4</sup>. Fitting the Arrhenius equation to the relaxation times  $\tau_{max}$ , allows the estimation of the activation energies  $E_A$  for the  $\beta$ -relaxation process of the different samples from the slope of the curves according to the Arrhenius equation

$$\tau_{max}(T) = \tau_{\infty} \exp\left[\frac{E_A}{RT}\right] \quad (\text{eq. S2})$$

with the universal gas constant R and infinite relaxation temperature  $\tau_{\infty}$ <sup>5</sup>. The activation energies were estimated 145 for the 6FDA-HAB and 115 and 120 and 65 kJ/mol for the 15%, 40%, and 100% allyl modifications, respectively. Values are in accordance with reported values for the beta relaxation of aromatic polyimides (130-160 kJ/mol)<sup>4,6,7</sup>.

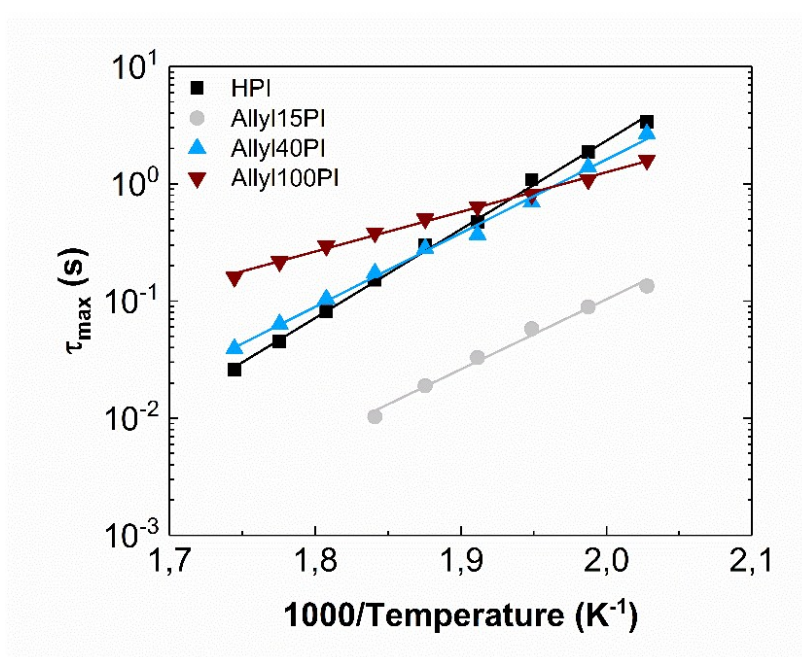


**Figure S11.** Relaxation times as a function of reciprocal temperature for the  $\beta$ -relaxation process. The symbols represent the experimental data 6FDA-HAB (■), Allyl15PI (●), Allyl40PI (▲) and Allyl100PI (▼). The solid lines represent the fitting curves according to the Arrhenius equation.

It has to be noted that the activation energies for the  $\beta$ -relaxation process varies significantly between the pristine material and the fully allylated polyimide. Since Allyl100PI contains no hydroxyl groups and therefore no hydrogen bonds between the polymer chains, and due to the spacer effect of the allyloxy unit (as seen by the increased d-spacing, see table 1), the polymer chain becomes more flexible, thus the activation energy for the relaxation process decreases, respectively. Additionally, these findings reveal, that the degree of allylation plays a crucial role to the onset and peak temperature of the  $\beta$ -relaxation process, which is in agreement to the trends of the TR temperature. There is also a strong correlation between the degree of allylation and the activation energy for the  $\beta$ -relaxation process (Figure S12). However, the trend for the  $\beta$ -relaxation activation energies does not follow the evolution of the TR temperature with respect to the degree of allylation (Figure S12).

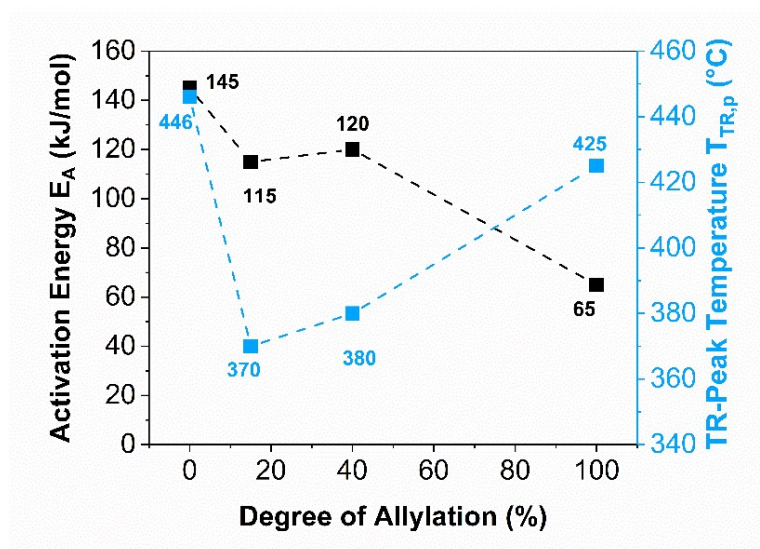


**Figure S12.** Determined activation energy of the  $\beta$ -relaxation (■), and the TR-peak temperatures of 6FDA-HAB, Allyl15PI, Allyl40PI and Allyl100PI (■) with respect to the degree of functionalization.

The relaxation times of the  $\gamma$ -relaxation process could not be described by the Arrhenius equation, with the fitting process being more inaccurate for Allyl15PI and Allyl40PI because these materials are copolymers containing different chemical species in the polymer backbone. Due to the complexity of the evaluation of these data and also since the  $\gamma$ -relaxation occurs in

a temperature range, that was not primarily responsible for the investigation of the TR process and it affects processes, this relaxation behavior was not investigated in more detail.

### Molecular weight and mechanical properties

**Table S3.** Apparent molecular weight ( $M_n$  and  $M_w$ ) and polydispersity ( $\bar{D}$ ) obtained by GPC (calibrated to PS-Standards), and mechanical properties determined by tensile test.

Degree of Allylation	Molecular Weight		$\bar{D}$	Tensile strength (MPa)	Tensile moduls (GPa)	Elongation at break (%)
	(kg mol <sup>-1</sup> )					
	$M_n$	$M_w$				
10	44	92	2.1	96.8	2270	6.4
15	47	132	2.8	54.9	1326	3.1
20	33	98	2.9	106.7	2084	8.2
40	79	199	2.5	97.5	1941	6.1
60	51	195	3.8	96.8	1967	6.2
80	53	241	4.5	86.3	2004	4.2
100	93	353	3.8	70.2	2833	2.7

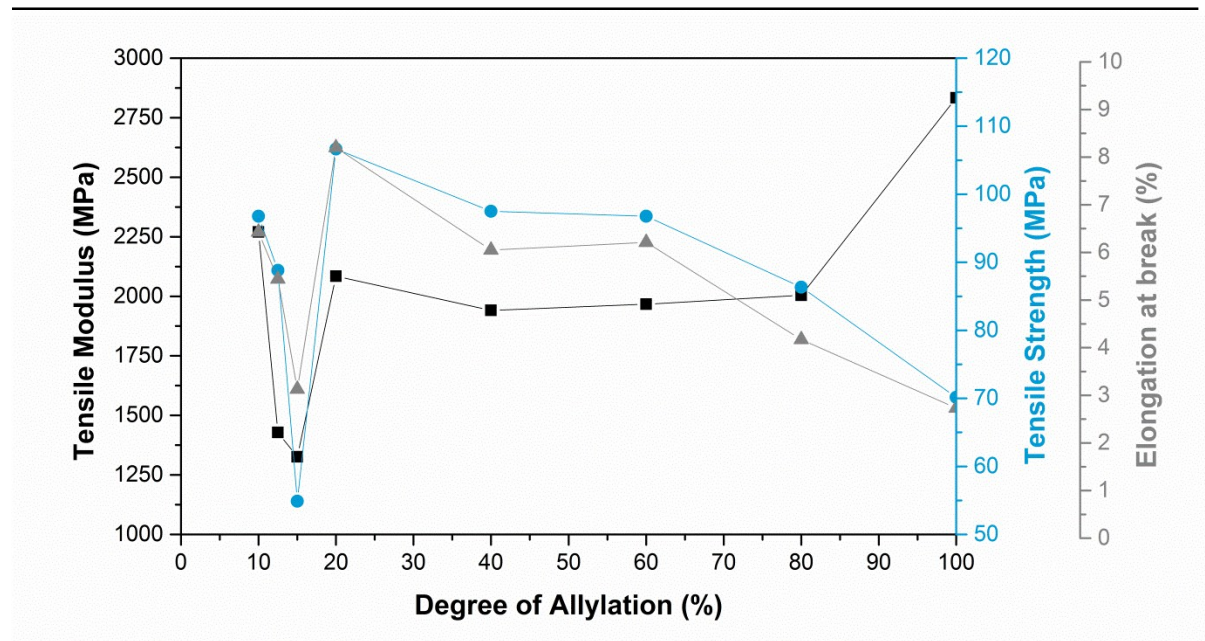


**Figure S13.** Mechanical properties obtained by tensile tests.

## Gas permeation measurements

### Permeability

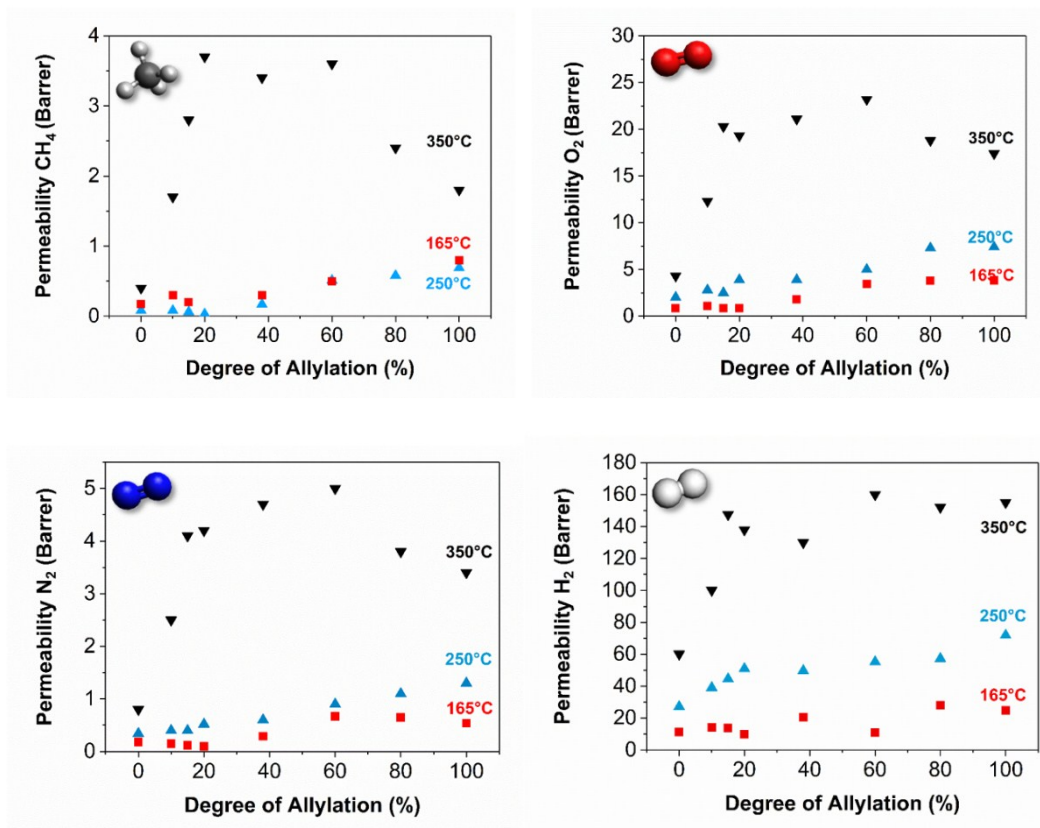


**Figure S14.** Permeability of different gases (CH<sub>4</sub>, O<sub>2</sub>, N<sub>2</sub>, H<sub>2</sub>) of the allylated polyimides after isothermal treatments of 165 °C, 250 °C and 350 °C versus degree of allylation.

## Selectivity

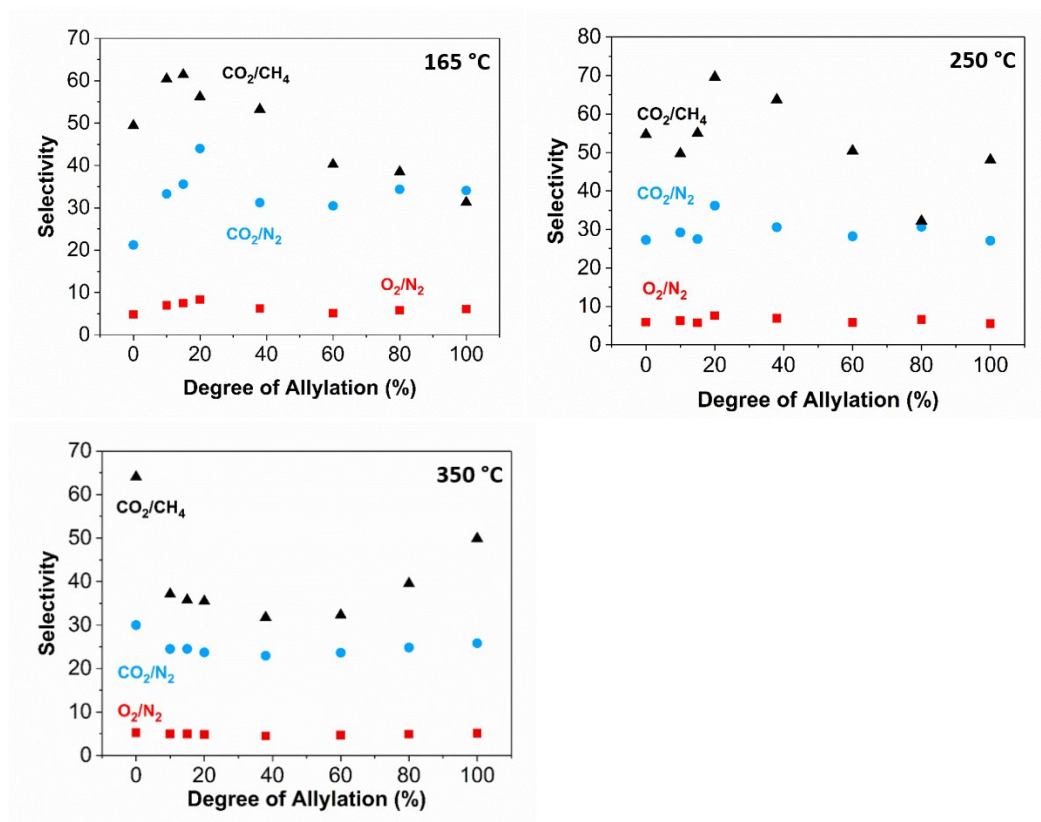


**Figure S15.** Selectivity of different gas pairs (CO<sub>2</sub>/CH<sub>4</sub>, O<sub>2</sub>/N<sub>2</sub>, CO<sub>2</sub>/N<sub>2</sub>) of the allylated polyimides after isothermal treatments of 165 °C, 250 °C and 350 °C versus degree of allylation.

**Table S4.** Permeability of different gases (CO<sub>2</sub>, CH<sub>4</sub>, O<sub>2</sub>, N<sub>2</sub>, H<sub>2</sub>) and selectivity of different gas pairs (CO<sub>2</sub>/CH<sub>4</sub>, O<sub>2</sub>/N<sub>2</sub>, CO<sub>2</sub>/N<sub>2</sub>) of the allylated polyimides after isothermal treatments of 165 °C and 250 °C versus degree of allylation.

Degree of Allylation	Permeability (barrer)						Ideal Selectivity		
	H <sub>2</sub>	He	N <sub>2</sub>	O <sub>2</sub>	CH <sub>4</sub>	CO <sub>2</sub>	O <sub>2</sub> /N <sub>2</sub>	CO <sub>2</sub> /CH <sub>4</sub>	CO <sub>2</sub> /N <sub>2</sub>
<b>0</b>									
<b>165 °C</b>	11.4	20.0	0.2	0.9	0.08	3.8	4.8	49.4	21.2
<b>250 °C</b>	27.2	36.7	0.3	2.0	0.17	9.4	5.9	54.7	27.3
<b>10</b>									
<b>165 °C</b>	14.3	21.6	0.2	1.1	0.08	5.1	6.9	60.4	33.3
<b>250 °C</b>	39.1	47.0	0.4	2.8	0.3	13.1	6.31	49.7	29.2
<b>15</b>									
<b>165 °C</b>	13.8	20.4	0.1	0.9	0.07	4.3	7.5	61.4	35.6
<b>250 °C</b>	44.6	52.6	0.4	2.5	0.2	11.0	5.7	55.0	27.5
<b>20</b>									
<b>165 °C</b>	10.0	17.3	0.1	0.8	0.08	4.5	8.3	56.2	44.0
<b>250 °C</b>	51.0	54.3	0.5	3.9	0.3	18.8	7.6	69.6	36.2
<b>40</b>									
<b>165 °C</b>	20.4	58.5	0.3	1.8	0.17	9.1	6.24	53.3	31.3
<b>250 °C</b>	49.7	54.8	0.6	4.2	0.3	18.9	6.85	63.7	30.6
<b>60</b>									
<b>165 °C</b>	11.0	31.8	0.7	3.5	0.5	20.5	5.15	40.3	30.5
<b>250 °C</b>	55.2	57.1	0.9	5.0	0.5	24.1	5.8	28.2	50.4

Degree of Allylation	Permeability (barrer)						Ideal Selectivity		
	H <sub>2</sub>	He	N <sub>2</sub>	O <sub>2</sub>	CH <sub>4</sub>	CO <sub>2</sub>	O <sub>2</sub> /N <sub>2</sub>	CO <sub>2</sub> /CH <sub>4</sub>	CO <sub>2</sub> /N <sub>2</sub>
<b>80</b>									
<b>165 °C</b>	28.1	30.3	0.6	3.8	0.6	22.3	5.8	38.5	34.4
<b>250 °C</b>	57.3	61.2	1.1	7.3	1.1	33.8	6.6	32.2	30.7
<b>100</b>									
<b>165 °C</b>	25.0	25.4	0.5	3.0	0.5	18.1	6.1	31.3	34.1
<b>250 °C</b>	71.9	69.7	1.3	7.4	0.8	36.3	5.5	48.1	27.1

## References

1. S. Havriliak and S. Negami, *Polymer*, 1967, **8**, 161-210.
2. P. Georgopoulos, V. Filiz, U. A. Handge and V. Abetz, *Macromolecular Chemistry and Physics*, 2016, **217**, 1293-1304.
3. T. Kollmetz, P. Georgopoulos and U. A. Handge, *Polymer*, 2017, **129**, 68-82.
4. M.-D. Damaceanu, V.-E. Musteata, M. Cristea and M. Bruma, *European Polymer Journal*, 2010, **46**, 1049-1062.
5. F. Kremer and A. Schönhal, *Broadband Dielectric Spectroscopy*, Springer Berlin Heidelberg, 2002.
6. A. C. Comer, D. S. Kalika, B. W. Rowe, B. D. Freeman and D. R. Paul, *Polymer*, 2009, **50**, 891-897.
7. M. Kochi, C. Chen, R. Yokota, M. Hasegawa and P. Hergenrother, *High Performance Polymers*, 2005, **17**, 335-347.